LOW-LOSS TUNING CIRCUITS FOR FREQUENCY-TUNABLE SMALL RESONANT ANTENNAS

Jani Ollikainen[1,2], **Outi Kivekäs**[1,3], **and Pertti Vainikainen**[1,4]

[1] Helsinki University of Technology, Institute of Digital Communications, Radio Laboratory,
P.O. Box 3000, FIN-02015 HUT, Finland,
E-mail: [2] jani.ollikainen@hut.fi, [3] outi.kivekas@hut.fi, [4] pertti.vainikainen@hut.fi

Abstract - Minimization of power loss in the tuning circuits of frequency-tunable small resonant antennas, such as microstrip patches, is studied. First, the frequency shift and the associated power loss in certain tuning circuits are theoretically calculated based on approximate circuit models of fairly narrow-band resonant antennas. By investigating the ratio of frequency shift and loss, an optimal configuration for the tuning circuit can be determined. The theoretical results can be used to provide optimal starting values and design curves that facilitate the final design with a full-wave electromagnetic simulator. To support the theory, a design procedure is demonstrated with two example antenna structures, for which both simulated and measured results are presented.

Keywords – Small antenna, frequency tuning, resonator, bandwidth, efficiency, and distortion

I. INTRODUCTION

One of the major application areas of small resonant antennas, such as short-circuited microstrip patch antennas or PIFAs (planar inverted-F antenna), is personal mobile communications. The main problem limiting the performance of these antennas is their narrow impedance bandwidth compared to their size. In some cases, the bandwidth problem can be alleviated with electrical frequency tuning [1], which increases the effective bandwidth and can enable e.g. the use of a single antenna element in several radio systems without increasing its size. Frequency-tunable antennas can be utilized e.g. in mobile communication terminals where small antenna size is currently one of the key requirements.

Besides more complex structure, power loss caused by the tuning circuitry is a major problem of frequency-tunable antennas [2]. Distortion caused by the non-linear components used as switches and electrically controlled reactances can also be a problem [3]. Previously, frequency-tunable patch antennas have been realized by connecting tunable reactances and switches directly between the patch and the ground plane [1], [4]. The same components have also been used to combine separate parts of the patch [5], [6]. The main emphasis in these studies has been on the achievable tuning range, whereas the power loss and distortion caused by the tuning circuit have received less attention.

In this paper, a simple but general frequency-tunable antenna configuration, which allows systematic analysis and minimization of power loss in the tuning circuit, is studied. In the first part, circuit models for single-resonant frequency-tunable patch antennas with a fairly narrow impedance bandwidth are used to develop formulas for the calculation of the frequency shift and the respective losses as a function of the parameters of the tuning circuit. By investigating the ratio of frequency shift and loss, an optimal configuration for the tuning circuit can be determined. In the second part, the theory is applied to the design of frequency-tunable shorted patch antennas.

II. THEORY

Near resonance, the impedance characteristics of a simple open-circuited or short-circuited patch antenna can be modeled with a parallel resonant circuit [7], [8] (Fig. 1). The resonant frequency of these antennas can be tuned up or down by adding an appropriate parallel susceptance. Ideally, any susceptance can be realized with a section of transmission line having length $\leq \lambda/2$ and a suitable termination. Two such transmission line sections connected by a single-pole single-throw (SPST) switch form a general tuning circuit that enables switching between two frequencies (f_{open} and f_{closed}). Besides the lengths of the transmission line sections, the obtained tuning range and the power loss in the tuning circuit depend on the coupling between the antenna and the tuning circuitry, which in turn depends on where the tuning circuit is connected to the antenna. This coupling can be modeled with an ideal transformer. With two sections of transmission line and an SPST-switch, four different tuning circuit configurations, covering all practical options, can be realized. The first two, shown in Fig. 1, comprise a series switch followed by a short-circuited or open-ended line. Two more can be obtained if the series switch in Fig. 1 is replaced with a shunt switch.

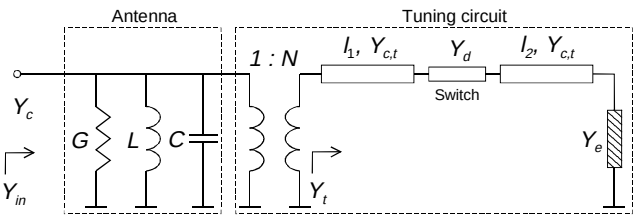

Fig. 1. *Circuit model for frequency-tunable resonant antenna with series switch. Load admittance Y_e represents the open ($Y_e = 0$) or shorted ($Y_e = \infty$) end of line 2.*

Near the resonant frequency f_r, the input admittance of a patch antenna (Fig. 1) without any tuning circuit can be approximated as:

$$Y_{in,a} = G\left[1 + j2Q_{0,a}\left(\frac{f - f_r}{f_r}\right)\right], \quad (1)$$

where $Q_{0,a}$ is the unloaded quality factor of the antenna. Assuming the antenna is matched at resonance, G can be replaced with Y_c, which is the characteristic admittance of the line feeding the antenna. The new resonant frequency f_i, obtained after adding a reactive load in Fig. 1, can be approximated from the frequency shift required for the antenna susceptance of Eq. (1) to cancel out the susceptance of the load:

$$\begin{aligned}&\mathrm{Im}\{Y_{in}\} = \mathrm{Im}\{Y_{in,a} + N^2 Y_t\} = \\ &2Y_c Q_{0,a}\left(\frac{f_i - f_r}{f_r}\right) + N^2 Y_{c,t} b_{L,i} = 0, \quad i = (open, closed).\end{aligned} \quad (2)$$

In Eq. (2), $Y_{c,t}$ is the characteristic admittance of the load line. The coupling between the antenna and the load line is described by N. The normalized susceptance of the load consisting of the switch and lines 1 and 2 is denoted by $b_{L,i}$. It can be calculated using the standard equations of lossy transmission lines and an equivalent circuit for the switch. Depending on the status of the switch, $b_{L,i}$ gets either the value $b_{L,open}$ or $b_{L,closed}$. The difference of the resulting frequencies gives the frequency shift:

$$\frac{\Delta f}{f_r} = \frac{f_{open} - f_{closed}}{f_r} = \frac{N^2}{2Q_{0,a}} \cdot \frac{Y_{c,t}}{Y_c} \cdot \underbrace{(b_{L,closed} - b_{L,open})}_{\text{Fig. 2c}} \quad (3)$$

The loss power of the load circuit of Fig. 1 is:

$$\begin{aligned}&P_{loss,t,i} = U_{in}^2 N^2 G_{L,i} = U_{in}^2 N^2 \,\mathrm{Re}\{Y_{L,i}\} = U_{in}^2 N^2 Y_{c,t} g_{L,i}, \\ &i = (open, closed).\end{aligned} \quad (4)$$

In Eq. (4), U_{in} is the input voltage of the antenna, and $g_{L,i}$ is the normalized real part of the load admittance. Assuming the antenna is matched at resonance ($G + G_L = Y_c$), the input power is $P_{in} = U_{in}{}^2 Y_c$. Now, the relative losses are:

$$\begin{aligned}&\frac{P_{loss,t,i}}{P_{in}} = \frac{N^2 Y_{c,t}}{Y_c}\mathrm{Re}\{y_{L,i}\} = \frac{N^2 Y_{c,t}}{Y_c} \cdot g_{L,i}, \\ &i = (open, closed).\end{aligned} \quad (5)$$

The frequency shift obtained with certain loss level or efficiency can be calculated as the ratio of Eqs. (3) and (5):

$$\frac{\Delta f / f_r}{P_{loss,t,i} / P_{in}} = \frac{1}{2Q_{0,a}} \cdot \underbrace{\frac{b_{L,closed} - b_{L,open}}{g_{L,i}}}_{\text{Figs. 2a and 2b}}, \; i = (open, closed). \quad (6)$$

It can be seen from Eqs. (3) and (4) that for a certain selection of the load circuit (l_1 and l_2), the increase of frequency shift by stronger coupling (increase of N) leads to a respective increase of power loss in the tuning circuit. However,

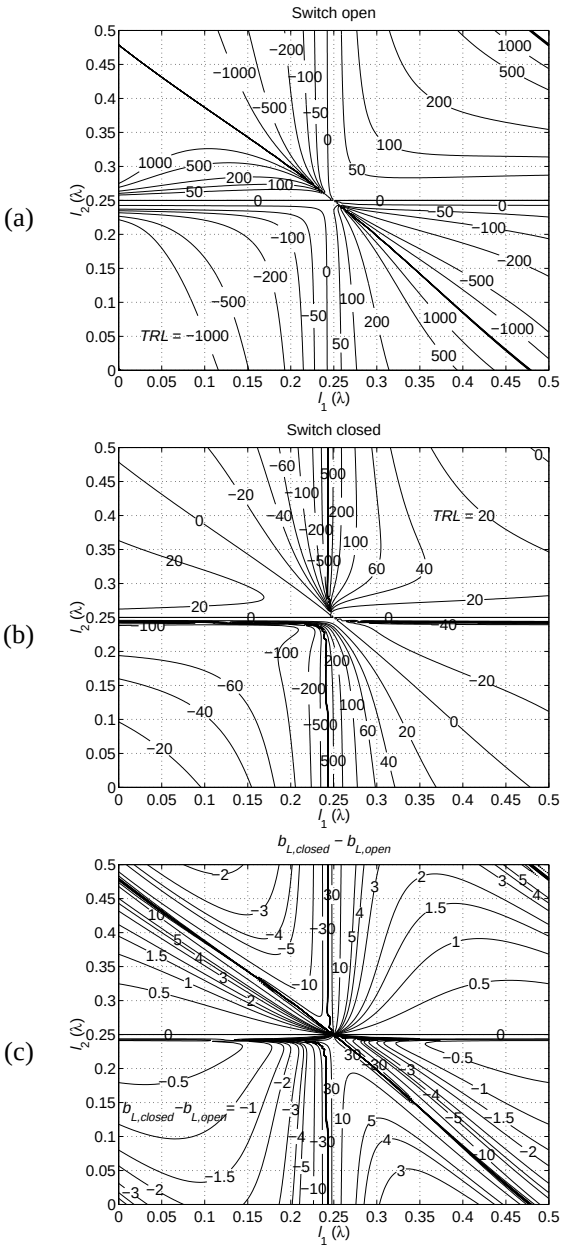

Fig. 2. *Normalized ratio of relative frequency shift and relative losses (TRL) for a) open and b) closed switch [Eq. (6)]. c) Normalized relative frequency shift [Eq. (3)]. Switch is connected in series, and the end of l_2 is short-circuited.*

for a given coupling, the ratio of the frequency shift and the associated power loss [Eq. (6)] can be maximized by selecting suitable lengths for the load lines. Therefore, it is useful to study the part of Eq. (6) that depends mainly on l_1 and l_2. It is here called the normalized ratio of frequency shift (or tuning range) over losses (*TRL*). Figs. 2a and 2b show *TRL* with the line lengths from 0 to 0.5λ for the open and closed switch, respectively. The tuning circuit is the more efficient, the larger the absolute values of *TRL* are. The signs just show the direction of tuning. Negative values represent cases where opening the switch decreases the frequency. Plots like

the ones in Figs. 2a and 2b can be used to quickly select optimal starting values for the design with electromagnetic simulators, and thus to reduce the number of iterations needed for an optimal design. The same plots can be used as design curves that facilitate e.g. the fine-tuning of a final design. When the power loss in the tuning circuit has been minimized by selecting suitable l_1 and l_2, the correct frequency shift can be set with the coupling coefficient N. The value of N can be calculated from Eq. (3), for which the normalized relative frequency shift ($b_{L,closed} - b_{L,open}$) can be read from Fig. 2c. Although N can be easily calculated based on the model, finding the correct coupling in the real structure typically requires few iteration rounds with an electromagnetic simulator.

Figs. 2a-2c have been plotted for the PIN-diode BAR 64-04W of Infineon. When reverse-biased (switch open), the PIN-diode was modeled as a 0.17 pF capacitor (reverse bias voltage V_R = 20 V). In forward-biased state (switch closed), it was modeled as a 1.2 nH inductor and a 2.1 Ω resistor in series (forward bias current I_F = 10 mA). Unless otherwise stated, the mentioned values for V_R and I_F are used in the rest of the paper. To simplify the calculations, it has been assumed that the impedances of the switch (in open and closed states) and the attenuation of the transmission lines 1 and 2 can be approximated with constant values within the moderate frequency tuning ranges used in this paper ($|\Delta f/f_r| \le 10$ %). In Fig. 2, the switch impedances have been calculated using the models given above at f = 900 MHz. The attenuation of the transmission lines is 0.07 dB/λ.

As a preliminary test for the calculated results, the model of Fig. 1 was studied with APLAC, which is an analog circuit simulation and design tool [9], [10]. The results given by APLAC were found to agree well with our calculations.

III. NARROW-BAND FREQUENCY-TUNABLE SHORTED PATCH ANTENNA (A1)

A. Design

To demonstrate the usefulness of the theoretical design curves of Fig. 2, a narrow-band frequency-tunable shorted patch antenna (A1), with a very high unloaded quality factor ($Q_{0,a}$ = 99) was designed. The high $Q_{0,a}$ was selected to represent a very difficult case to tune. As the theoretical ratio of frequency shift and loss is inversely proportional to $Q_{0,a}$ [Eq. (6)], any antenna with $Q_{0,a} < 99$ can be tuned an equal amount with less power lost in the tuning circuit. The tuning range was selected to be approximately 5 % and the direction of tuning so that f_r increases as the switch is closed ($\Delta f/f_r$ = –0.05). The PIN-diode described in Sec. II was used as the switch. A simple short-circuited patch antenna, with f_r around 900 MHz, was chosen as the test structure. It was mounted on a large 0.3 m × 0.3 m ground plane to enable radiation efficiency measurement with the Wheeler cap method [11], [12]. The high $Q_{0,a}$ for the test antenna was obtained by making it very thin.

The antenna element without the tuning circuit (f_r = 957 MHz and $Q_{0,a}$ = 99) was first designed with a commercial method-of-moments (MoM) -based full-wave electromagnetic simulator (IE3D). After that suitable line lengths l_1 and l_2 were approximated based on Fig. 2 and similar figures for the three other possible tuning circuit configurations. Owing to the largest ratio of tuning range over losses (*TRL*) with the shortest combined length of l_1 and l_2, the tuning circuit comprising a series switch and a short-circuited line 2 was selected. The goal was to minimize the power loss in the tuning circuit while keeping it approximately equal in both switching states. The line lengths l_1 = 0.21λ and l_2 = 0λ (at 957 MHz) were selected as starting values. As shown in Fig. 2, this leads to the *TRL* ≈ –120 in both states of the switch. If l_1 is increased from 0.21λ, *TRL* increases in the closed state of the switch but decreases in the open state. Thus, the chosen line lengths can be regarded as optimal. After selecting the starting values for l_1 and l_2, a coupling coefficient (N) giving the frequency shift of 5 % was determined from Eq. (3). The value N = 1.4 was obtained by substituting: Q_a = 99, f_r = 957 MHz, $\Delta f/f_r$ = –0.05, $Y_{c,t} = Y_{c,}$ = 20 mS, and $b_{L,closed} - b_{L,open}$ = –5.1.

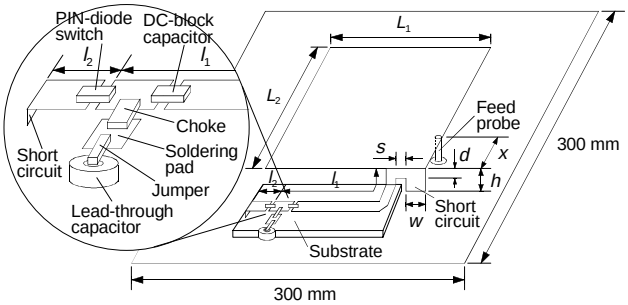

Fig. 3. *Geometry of frequency-tunable shorted patch antenna.*

The final antenna structure, including the tuning circuit and a DC-control circuit for the switch, was designed with IE3D (Fig. 3). In the simulations, air was used as the dielectric for the antenna and for the tuning circuit. For the prototype, the tuning circuit was scaled for 0.79 mm-thick RT/duroid 5870 substrate ($\varepsilon_r' = 2.33$ and $\tan\delta = 0.0012$). The tuning circuit was positioned beside the antenna for easier prototyping. However, it is also possible to position it between the patch and the ground plane in order to save space. The patch was made of tin bronze, whereas the tuning lines and the ground plane were made of copper. To reduce the computation time, the 0.3 m × 0.3 m ground plane was approximated in the simulations with an infinite ground plane. The main dimensions of the antenna in millimeters are: L_1 = 43.4, L_2 = 43.5, h = 3, w = 5.4, x = 2.5, d = 0, s = 0.5. The final lengths of the tuning lines were l_1 = 42.3 mm (0.18λ at 912 MHz, including the pin connecting line 1 and the patch) and l_2 = 5.3 mm (0.02λ at 912 MHz). Only minor changes to the preliminary dimensions were required to obtain the desired performance. The slight increase of l_2 from zero was done to make it easier to attach the switch to the tuning circuit.

Based on the design curves of Fig. 2, this was expected to have a negligible effect on the performance.

B. Results

Fig. 4 shows the simulated and measured frequency responses of reflection coefficient for the optimized antenna with the switch open, with the switch closed, and with the tuning circuitry removed. A good agreement between the simulated and measured results can be observed. The simulated frequency shift is from f_r = 911 MHz (switch open) to f_r = 959 MHz (switch closed, 5.3 %), whereas the measured frequency shift is from f_r = 912 MHz to f_r = 957 MHz (5.0 %).

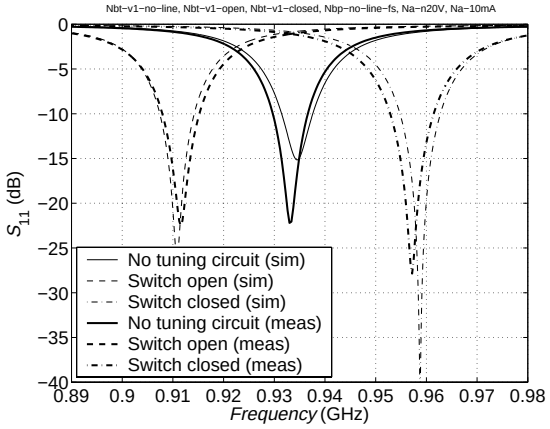

Fig. 4. *Simulated and measured frequency responses of reflection coefficient for A1.*

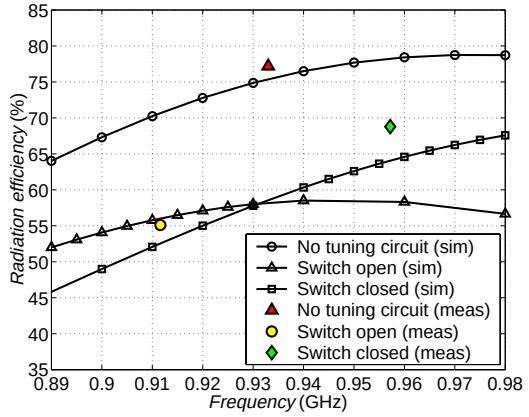

Fig. 5. *Simulated and measured radiation efficiencies for A1.*

Fig. 5 presents the simulated and measured radiation efficiencies. The efficiency measurements were performed with the Wheeler cap method [11], [12]. As shown in Fig. 5, the simulated and measured efficiencies agree very well. The simulated efficiency of the antenna without the tuning line is fairly low and changes considerably with frequency. This is a well-known problem of thin (here $0.009\lambda_0$) microstrip patch antennas. Although the used antenna element is not the best choice for practical applications, it is fully appropriate for the study of losses caused by the tuning circuit. To show only the effect of losses caused by the tuning circuit, the simulated and measured radiation efficiencies with the tuning circuit have been normalized to the respective simulated and measured radiation efficiencies without the tuning circuit (Table 1). The measured cases were normalized to the simulated efficiency curve without the tuning circuit after its level had been corrected so that it passed through the value measured without the tuning circuit.

Table 1.
Normalized simulated and measured radiation efficiencies for A1. Simulated values given in the range $f_r \pm 5$ MHz.

	Switch open	**Switch closed**
Simulated	79…80	81…83
Measured	76	86

Distortion generated by the non-linear tuning element can be a problem in frequency-tunable antennas. Therefore, the linearity of the prototype was studied with the two-tone intermodulation distortion measurement. When the switch was closed, no measurable intermodulation (IM) products were observed. At the input power level P_{in} = 30 dBm/tone, the level of third-order intermodulation products (IMD_3) was below –80 dBc and the third-order input intercept point IIP_3 > 70 dBm. When the switch was opened, the distortion increased considerably and IIP_3 decreased to 46 dBm. Reduction of V_R was found to increase the distortion. When V_R was reduced to 3 V and 0 V, IIP_3 decreased to 40 dBm and 30 dBm, respectively. The generation of harmonic frequencies was studied at the input power level P_{in} = 33 dBm. The level of harmonics was found to be below –85 dBc in both states of the switch. When V_R in the open state was reduced to 0 V, the first and second harmonic increased to –73 dBc and –74 dBc, respectively.

IV. FREQUENCY-TUNABLE SHORTED PATCH ANTENNA FOR E-GSM900 (A2)

A. Design

A prototype that is capable of switching between the transmitting (TX, 880…915 MHz) and receiving (RX, 925…960 MHz) band of an E-GSM900 mobile station (MS) and has the adequate bandwidths and a high radiation efficiency at both bands is presented as the second example (A2). The same PIN-diode switch (BAR 64-04W) was used as in the first example. The goal was to minimize the power loss in the tuning circuit and to obtain approximately equal radiation efficiencies at both bands.

The antenna is based on a shorted patch with Q_0 = 20 and f_r = 900 MHz. A tuning circuit comprising a series switch and a short-circuited line 2 was selected also for this design. The direction of tuning was chosen to be the opposite to that of the first example so that f_r decreases when the switch is closed. In this case, the correct tuning direction is obtained with positive *TRL*-values. Selecting $l_1 = 0.28\lambda$ and $l_2 = 0.02\lambda$

leads to $TRL = 100$. This choice gives the largest common *TRL*-value with the shortest total line length. After finding optimal starting values for l_1 and l_2, the coupling coefficient that gives the correct frequency shift was determined from Eq. (3). The value $N = 0.6$ was obtained by substituting: $Q_a = 20$, $f_r = 900$ MHz, $\Delta f/f_r = 0.05$, $Y_{c,t} = Y_c = 20$ mS and $b_{L,closed} - b_{L,open} = 5.0$. The obtained N is smaller than that obtained in the previous example. This means that the tuning circuit must be connected to the antenna relatively closer to the point of zero impedance than in the first example. The final antenna structure was designed with IE3D and constructed the same way as in the first example. Its main dimensions in millimeters are: $L_1 = 46.7$, $L_2 = 46.6$, $h = 12$, $w = 10$, $x = 7.5$, $d = 6$, $s = 1.9$ (Fig. 3). The final lengths of the tuning lines were $l_1 = 60.3$ mm (0.25λ at 941 MHz, including the pin connecting line 1 and the patch) and $l_2 = 5.0$ mm (0.02λ at 941 MHz).

B. Results

Fig. 6 shows a good agreement between the simulated and measured frequency responses of reflection coefficient for the optimized antenna. In simulations, the resonant frequency shifted from 941 MHz down to 897 MHz (4.7 %), whereas the measured shift is from 941 MHz to 898 MHz (4.6 %). The measured antenna covers the TX and RX bands of an E-GSM900 mobile station with the return loss $L_{retn} \geq 8.5$ dB.

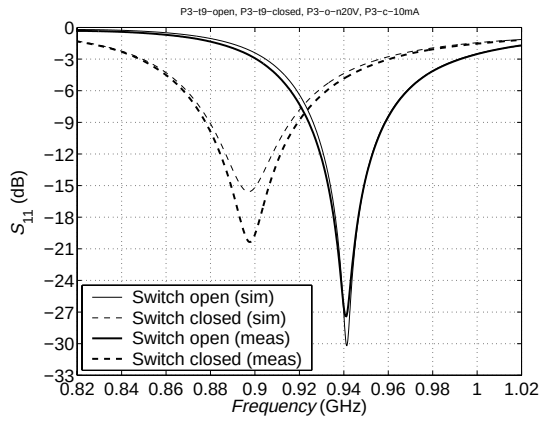

Fig. 6. *Simulated and measured frequency responses of reflection coefficient for A2.*

Fig. 7 shows the simulated and measured (Wheeler cap) radiation efficiencies for the antenna. The measured radiation efficiencies are 95 % at both resonant frequencies. Reducing either the reverse bias voltage V_R or forward bias current I_F from the original design values of $V_R = 20$ V (switch open) and $I_F = 10$ mA (switch closed) was found to decrease the efficiency. When V_R was reduced to 0 V, the efficiency decreased to 92 %. When I_F was reduced to 1 mA, the efficiency decreased to 88 %. This is a small decrease considering that the reduction of I_F increased the typical forward resistance of the PIN-diode from 2.1 Ω to 12.5 Ω. The resonant frequencies did not change appreciably. To show only the effect of losses caused by the tuning circuit, the simulated and measured radiation efficiencies with the tuning circuit have been normalized to the respective simulated and measured radiation efficiencies without the tuning circuit the same way as in the first example (A1). The normalized values are shown in Table 2.

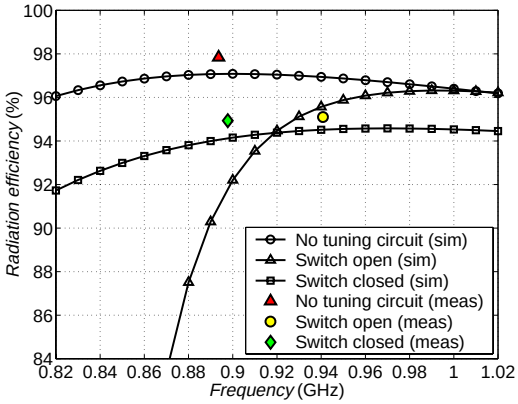

Fig. 7. *Simulated and measured radiation efficiencies for A2.*

Table 2.
Normalized simulated and measured radiation efficiencies for A2. Simulated values given in the range $f_r \pm 20$ MHz.

	Switch open	**Switch closed**
Simulated	97	97…99
Measured	97	97

The linearity of the second prototype was also studied with the two-tone test. When the switch was closed, no measurable intermodulation products were observed (with $P_{in} = 30$ dBm/tone $IMD_3 < -80$ dBc and $IIP_3 > 70$ dBm). When the switch was opened, the distortion increased and IIP_3 decreased to 61 dBm. Reducing the reverse bias to 3 V and 0 V, increased the distortion and decreased IIP_3 to 53 dBm and 40 dBm, respectively. The generation of harmonic frequencies was studied at the input power level $P_{in} = 33$ dBm. The level of harmonics was below –85 dBc in both states of the switch. When the reverse bias was reduced to $V_R = 0$ V in the open state, the level of the first harmonic increased to –69 dBc, whereas the second one stayed below –85 dBc.

In simulations, adding the tuning circuit was found to have only a minor effect on the radiation patterns of both prototypes (A1 and A2). The effect was the largest when the switch was open.

V. CONCLUSIONS

A design method for single-resonant frequency-tunable patch antennas has been proposed. By using the presented method the power loss in the frequency tuning circuit can be systematically minimized with respect to the achievable tuning range between two frequencies. As application examples, two frequency-tunable shorted patch antennas were de-

signed. In electromagnetic simulations, the first antenna with $Q_{0,a} = 99$ was tuned 5.3 % with the losses of the tuning circuitry reducing the radiation efficiency roughly by 20 % at both frequencies. The measured tuning range was 5.0 %, while the losses of the tuning circuitry reduced the efficiency by 24 % at the lower frequency and by 14 % at the higher frequency. With the proposed method, a moderate frequency tuning ($\Delta f/f_r \approx 5$ %) of even a very narrow-band antenna can be done with fairly small reduction of efficiency caused by the tuning circuit. The second antenna with $Q_{0,a} = 20$ was designed for switching between the TX and RX bands of an E-GSM900 mobile station. Both in simulations and in measurements, the necessary frequency tuning was obtained at the expense of roughly 3 % reduction in efficiency. With both prototypes, the efficiency was found to decrease as either the reverse bias voltage or the forward bias current was decreased. According to the presented theory [see Eq. (6)], the ratio of frequency shift and the associated power loss in the studied tuning circuits is inversely proportional to $Q_{0,a}$. Therefore, an antenna with a wide bandwidth (low $Q_{0,a}$) can be tuned a given amount with higher efficiency than an antenna with a narrow bandwidth (high $Q_{0,a}$). Alternatively, it is possible to obtain a larger tuning range instead of a higher efficiency. The designed examples and measured results clearly support the theory.

The tuning circuits of both prototypes caused very little distortion when the switch was closed ($IIP_3 > 70$ dBm). Opening the switch increased the distortion, which was found to depend on the applied reverse bias. In both cases, the distortion increased as the reverse bias was decreased. At 20 V reverse bias, the antenna with $Q_{0,a} = 20$ was found to be more linear ($IIP_3 = 61$ dBm) than the one with $Q_{0,a} = 99$ ($IIP_3 = 46$ dBm).

ACKNOWLEDGEMENTS

This research was funded by Nokia Mobile Phones. The authors would like to thank I. Pankinaho, A. Lehtola, and J.-P. Louhos for fruitful technical discussions. The postgraduate studies of the first two authors have been financially supported by the Academy of Finland, the Graduate School in Electronics, Telecommunications, and Automation (GETA), Tekniikan Edistämissäätiö (TES), The Finnish Society of Electronics Engineers (EIS), Nokia Foundation, Ulla Tuominen Foundation, and Emil Aaltonen Foundation. All the supporters are warmly thanked.

REFERENCES

[1] P. Bhartia and I. J. Bahl, “Frequency agile microstrip antennas,” *Microwave J.*, Vol. 25, No. 10, Oct. 1982, pp. 67-70.

[2] R. B. Waterhouse and N. V. Shuley, ”Full characterisation of varactor-loaded, probe-fed, rectangular, microstrip patch antennas,” *IEE Proc.-Microw. Antennas Propag.*, Vol. 141, No. 5, Oct. 1994, pp. 367-373.

[3] C. Kalialakis, P. Gardner, and P. S. Hall, “Harmonic radiation from varactor-loaded microstrip antennas,” *Proc. 31st European Microwave Conference (EuMC2001)*, Vol. 2, London, UK, Sept. 25-27, 2001, pp. 133-136.

[4] P. K. Panayi, M. O. Al-Nuaimi, and L. P. Ivrissimtzis, “Tuning techniques for planar inverted-F antenna,” *Electronics Lett.*, Vol. 37, No. 16, Aug. 2001, pp. 1003-1004.

[5] K. L. Virga and Y. A. Rahmat-Samii, “Low-profile enhanced-bandwidth PIFA antennas for wireless communications packaging,” *IEEE Trans. Microwave Theory Tech.*, Vol. 45, No. 10, Oct. 1997, pp. 1879-1888.

[6] F. Yang and Y. Rahmat-Samii, “Patch antenna with switchable slot (PASS): dual-frequency operation,” *Microwave and Opt. Tech. Lett.*, Vol. 31, No. 3, Nov. 5, 2001, pp. 165-168.

[7] W. F. Richards, Y. T. Lo, and D. D. Harrison, “An improved theory for microstrip antennas and applications,” *IEEE Trans. Antennas Propagat.*, Vol. 29, No. 1, Jan. 1981, pp. 38-46.

[8] T. Taga, “Analysis of planar inverted-F antennas and antenna design for portable radio equipment,” Chapter 5 in *Analysis, Design, and Measurement of Small and Low-Profile Antennas*, K. Hirasawa and M. Haneishi, (Eds.), Boston, 1992, Artech House, 270 p.

[9] M. Valtonen, “APLAC – Object-oriented circuit simulation and design tool,” *Proc. Microwave and RF Conference ´97*, London, UK, Sept. 30 - Oct. 2, 1997.

[10] Web page of APLAC Solutions, available in <URL: http://www.aplac.com/> [cited July 1, 2002].

[11] H. A. Wheeler, “The radiansphere around a small antenna,” *Proc. IRE*, Vol. 47, No. 8, Aug. 1959, pp. 1325-1331.

[12] D. M. Pozar and B. Kaufman, “Comparison of three methods for the measurement of printed antenna efficiency,” *IEEE Trans. Antennas Propagat.*, Vol. 36, No. 1, Jan. 1988, pp. 136-139.